

RLVR Datasets and Where to Find Them: Tracing Data Lineage for Better Training Data

Hsiu-Yuan Huang^{1,2,3}, Weijie Liu^{3*}, Chenming Tang^{1,2}, Sanwoo Lee^{1,2},
Kai Yang³, Yangkun Chen³, Saiyong Yang³, Yunfang Wu^{1,2*}

¹National Key Laboratory for Multimedia Information Processing, Peking University

²School of Computer Science, Peking University

³LLM Department, Tencent

✉ huang.hsiuyuan@stu.pku.edu.cn, wuyf@pku.edu.cn

Abstract

The proliferation of Reinforcement Learning from Verifiable Rewards (RLVR) datasets has exacerbated provenance collapse due to unclear lineage among existing datasets. To bridge this fragmented RLVR data landscape, we propose Atomic-source Tracing via Lineage-Aware Search (ATLAS), a systematic framework for tracing RLVR datasets back to their atomic sources, attributing over 99.7% of 1.45M instances to 20 atomic sources. Our analysis reveals that most RLVR datasets are variants of a small set of shared upstream sources, with few introducing genuinely new data, and many facing data contamination risks. These findings naturally motivate us to curate a new RLVR dataset, DAPO++, and to benchmark existing datasets from a lineage-aware perspective. To this end, we propose Source-level Counterfactual Attribution (SCA) as a guiding principle to curate a decontaminated training dataset with concentrated learning signals. Essentially, SCA measures a sample’s marginal utility by comparing per-atomic-source RL checkpoints against a shared base model. Building upon these attribution signals, we further design a composite dataset quality score Q that strongly correlates with downstream RLVR performance. Experiments on Qwen3 series models verify that DAPO++ consistently improves performance on held-out benchmarks, while Q reliably predicts downstream RLVR training effectiveness. Our code and data is available at <https://github.com/Celine-hxy/ATLAS>.

1 Introduction

Where Do We Come From? What Are We? Where Are We Going? —Paul Gauguin

The emergence of Reinforcement Learning from Verifiable Rewards (RLVR) has driven rapid growth in both RLVR research and training corpora. Existing studies have investigated RLVR from var-

* Corresponding author.

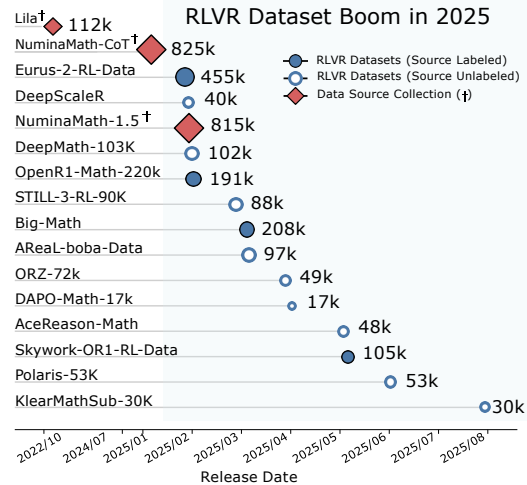


Figure 1: Timeline of RLVR dataset releases. The field has grown rapidly since 2025, with many datasets being “*openly-closed*”, meaning that although the datasets are publicly available, their underlying data provenance remains opaque.

ious perspectives, including model behavior, optimization dynamics, and data attribution (Yan et al., 2025; Zhou et al., 2026). However, these works are often trained and evaluated on substantially different datasets, making empirical results difficult to compare fairly. Meanwhile, the rapid proliferation of RLVR datasets (Figure 1), many of which lack clear provenance or source annotation, has raised a practical yet underexplored question: *where do these RLVR datasets come from, and how can we find better datasets for RLVR training?*

One of our goals is to trace data back to its *atomic sources*, namely the original points of collection or construction (e.g., a specific book, website, competition, or crowdsourced effort), rather than merely tracing datasets back to their immediate predecessors. This is motivated by our finding that modern RLVR datasets are often built upon prior datasets through filtering, rewriting, recombination, and iterative aggregation, resulting in sub-

stantial overlap across datasets (§ 2.2). We argue that atomic-source tracing provides the following perks: (1) **“Where Do We Come From”—tracing errors, synthetic data, and leakage:** data lineage tracing improves dataset transparency by disentangling the hidden composition of *openly-closed* datasets (Figure 1), making it possible to address *provenance collapse* (Brooks, 2025), namely the loss of information about where data came from, who modified it, and whether it can be trusted. (2) **“What Are We”—encouraging quality-oriented data development:** provenance tracing reduces repetitive data cleaning and saves human and computational resources, enabling greater focus on high-quality data construction. (3) **“Where Are We Going”—exploring uncharted data sources:** understanding existing data provenance helps reveal which domains remain underexplored, providing guidance for future data mining. To address these, we propose an *Atomic-source Tracing via Lineage-Aware Search* (ATLAS) framework (§ 2.1), through which we trace 1,450,827 RLVR instances back to 20 atomic data sources and provide detailed analysis (§ 2.2), including million-scale pairwise similarity matching against 14 mathematical evaluation benchmarks to detect leakage, uncovering 36,148 leaked instances across datasets. Insights derived from ATLAS further motivate us to curate a new RLVR dataset DAPO++.

Another goal of this work is to systematically benchmark existing RLVR datasets, thereby providing a roadmap for the dataset construction and selection, both of which constitute a fundamental prerequisite for RLVR research. Built upon ATLAS, we further propose *Source-level Counterfactual Attribution* (SCA), a source-aware attribution framework that enables learnability annotation and source-level utility estimation (§ 3.1). Together, ATLAS and SCA form the foundation of our RLVR dataset benchmarking and scoring framework (§ 3.2), enabling systematic ranking and analysis of existing RLVR datasets.

Our contributions can be summarized as follows:

- We propose ATLAS, a data lineage tracing framework for RLVR datasets, and provide detailed analyses of dataset provenance and benchmark leakage, and curate a new dataset DAPO++, based on the insights derived from our analysis.
- Built upon ATLAS, we propose **Source-level Counterfactual Attribution (SCA)**, a source-

aware attribution method that estimates the contribution of atomic data sources to RLVR training effectiveness while providing fine-grained instance-level learnability annotations.

- Leveraging ATLAS and SCA, we systematically benchmark existing RLVR datasets, to support future RLVR training and dataset construction.

2 RLVR Dataset Lineage and Provenance

To facilitate the discussion of our *Atomic-source Tracing via Lineage-Aware Search* (ATLAS) framework for RLVR training corpora, we first clarify the key concepts and terminology involved.

- **Data Source:** A collection of instances not intended for RLVR training. If its origin is singular or its data follow a consistent standard, it is referred to as an *atomic source*.
- **Dataset:** A general term for a collection of data that may aggregate instances, data sources, or other datasets. In this paper, it mostly refers to the data collection associated with a HuggingFace dataset identifier.
- **RLVR Dataset:** A dataset specifically constructed for RLVR training, whose contents are typically composition of multiple data sources.

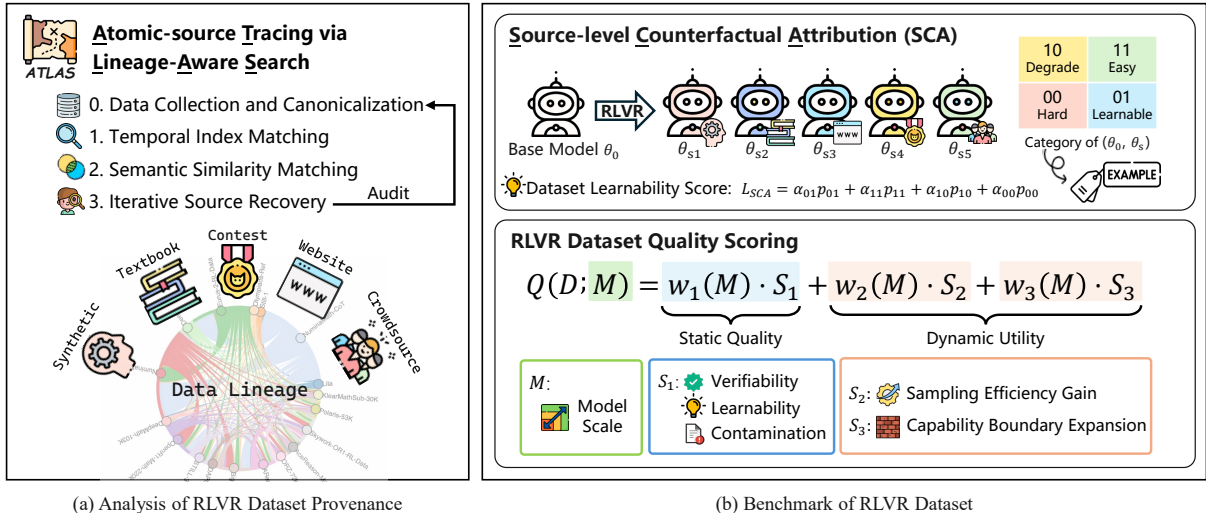
2.1 ATLAS Framework

Our ATLAS framework is illustrated in Figure 2(a), while the corresponding pseudocode is presented in Appendix A.2. And detailed discussions of related work are provided in the Appendix D, due to space limitations.

Stage 0: Data Collection and Canonicalization.

We collect a set of commonly used RLVR datasets from the open-source community, along with the upstream datasets on which they are built, forming the initial seed dataset pool for source tracing. Detailed descriptions of the manually collected and thoroughly inspected datasets, which constitute the core infrastructure of our study, are provided in Table 6, including release dates, Hugging Face IDs, dataset sizes, associated papers, and Hugging Face links.

Due to substantial heterogeneity across datasets, including schema, storage formats, and prompt



(a) Analysis of RLVR Dataset Provenance

(b) Benchmark of RLVR Dataset

Figure 2: Overview of our framework for RLVR dataset provenance analysis and benchmarking.

structures, data canonicalization is non-trivial and typically requires manual inspection. For example, a single dataset may append multiple instructions of varying formats after each prompt. To address this, we manually inspect each dataset by sampling 30 to 50 instances, from which we extract and standardize the final question-answer pairs.

Stage 1: Temporal Index Matching. To efficiently determine the occurrence status of a given prompt, we design a hash-based temporal indexing mechanism that avoids costly string-level matching. For each prompt p , we compute a 40-character hexadecimal identifier h using *SHA-1* hashing, enabling efficient lookup across datasets. We then traverse all instances in chronological order while maintaining a global lineage dictionary $\mathcal{L}[h]$ which stores instance metadata together with the occurrence list $\mathcal{O}[h]$, and update the record accordingly with metadata when provided.

Stage 2: Semantic Similarity Matching. To recover source attribution for instances unresolved by exact matching, we perform semantic similarity matching over the unmatched set \mathcal{U} , where mismatches often arise from prompt-level transformations. Specifically, we encode the entire corpus using Sentence-BERT embeddings (Reimers and Gurevych, 2019) and trace unmatched instances back to their potential source data through cosine similarity retrieval under human auditing, in which we manually verify them case-by-case and judge whether they match.

Stage 3: Iterative Source Recovery. We manually inspect their question types and formatting

patterns to identify potential missing sources, if the number of unmatched instances in \mathcal{U} exceeds a threshold τ . Based on these observations, we select candidate datasets \mathcal{D}_{new} from potential repositories, primarily authoritative releases not yet included in data sources, incorporate them into the global dataset pool, and rerun Stage 0–2 matching. Subsequently, candidate datasets \mathcal{D}_{new} that fail to recover meaningful matches are discarded from the dataset pool. This iterative process continues until the number of unmatched instances in \mathcal{U} falls below τ . The remaining unmatched instances are labeled as *unknown*.

2.2 RLVR Dataset Provenance

In our implementation, we set the $\tau = 1\%$, and the final lineage dictionary contains 1,450,827 instances, with fewer than 1% labeled as *unknown*.

Source Decomposition. Figure 3 presents the atomic-source decomposition of representative RLVR training datasets traced by our ATLAS framework, while Figure 5 (Appendix A.3) further reveals the specific RLVR datasets in which these atomic data sources were first introduced. Although many datasets exhibit substantial atomic source overlap, we still observe considerable heterogeneity in the relative source proportions across datasets.

Dataset Contribution. We further visualize the compositional relationships among RLVR datasets using Bokeh plots, as shown in Figure 2(a), where the detailed views for each dataset are provided in Appendix A.3. Moreover, Eurur-2-RL-Data makes

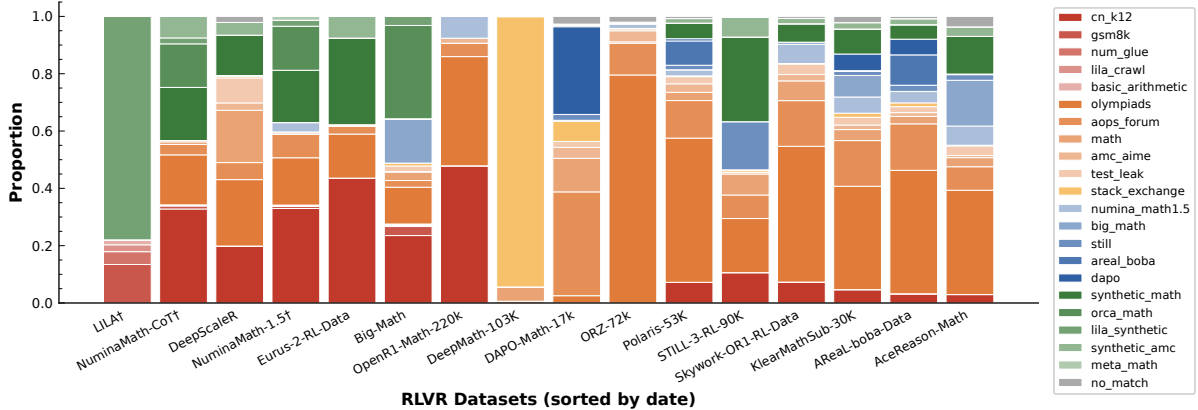


Figure 3: Atomic-source composition and relative proportions. Major source datasets are marked with †. We manually annotate each atomic source with a problem-type label and group them into several color-coded categories, as detailed in Table 7. Within each type, larger atomic sources are represented using darker shades.

a notable contribution by extensively cleaning and transforming the MCQs in NuminaMath-CoT into open-ended reasoning formats, which were proven effective (§ 4.2) and were subsequently inherited by a large number of later RLVR datasets.

Dataset Leakage Risk Analysis We conduct large-scale *exhaustive pairwise similarity matching* between RLVR datasets and commonly used evaluation benchmarks to analyze potential benchmark leakage between existing RLVR datasets (Figure 4), major source datasets (Appendix B.1), and commonly used evaluation benchmarks. Our analysis reveals three major concerns, with detailed cases provided in Appendix B.2. (1) We identify several RLVR datasets that directly include benchmarks originally proposed for RLVR evaluation as part of their training data, such as OmniMath and HARP, leading to explicit contamination. (2) Through similarity-based matching, we find that benchmark leakage is pervasive across current RLVR datasets. In many cases, the leaked instances differ from benchmark test samples only in superficial formatting variations (Case 1, 2 and 3), making such leakage difficult to detect through conventional rule-based filtering. (3) We further observe cases where benchmark instances are lightly modified or partially rewritten while still retaining extremely high semantic overlap with the original test problems (Case 4), posing substantial hidden leakage risks.

It should be emphasized that results in Figure 4 only cover high-confidence leakage cases (similarity $\geq 90\%$). We nevertheless observe substantial leakage at lower similarity levels

(e.g., similarity $\approx 80\%$), particularly for MCQ-transformed variants with nearly identical underlying content, suggesting that the reported results may still underestimate the true extent of benchmark contamination. This calls for a more rigorous provenance tracking and leakage auditing, and further raise an important question: *how does contamination affect the utility and downstream performance of RLVR datasets?*

3 Benchmarking RLVR Datasets

In this section, we address the above question by proposing a multi-dimensional dataset quality scoring framework for benchmarking RLVR datasets, as illustrated in Figure 2(b). We first introduce *Source-level Counterfactual Attribution* (SCA), a data attribution method built upon the atomic sources identified by ATLAS. SCA enables instance-level learnability labeling, which subsequently serves as a key component of our scoring framework.

3.1 Source-level Counterfactual Attribution

A central challenge in evaluating RLVR training data is that the contribution of an individual instance cannot be directly isolated, as RL training is a global optimization process where the effect of each sample is heavily entangled with the overall training distribution (Koh and Liang, 2020; Ghorbani and Zou, 2019; Hu et al., 2025b). To address this, we propose SCA, a data attribution method that operates at the granularity of atomic sources from ATLAS (§ 2.1). Specifically, SCA treats data instances from the same atomic source, whose shared origins and annotation protocols make them

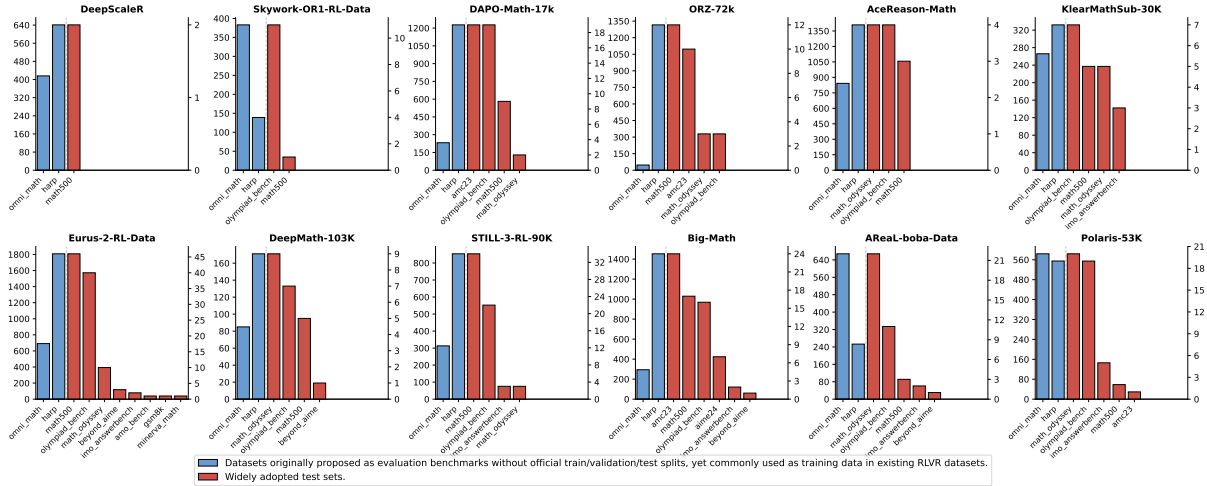


Figure 4: Leakage severity of RLVR datasets measured by semantic similarity to benchmark test sets.

more likely to exhibit similar stylistic and domain characteristics, as a single intervention unit to reduce attribution confounding. For each atomic source s , we train a corresponding RL checkpoint θ_s , initialized from the base model θ_0 , thereby forming a counterfactual pair (θ_0, θ_s) . By evaluating instances $i \in s$ on both θ_0 and θ_s , the resulting behavioral difference provides a minimally confounded proxy for estimating the contribution of individual instances to RLVR training.

We further perform a one-time binary labeling by comparing the correctness outcomes of (θ_0, θ_s) on each instance, yielding four categories (00, 01, 10, 11) that characterize different levels of instance learnability. Specifically, 00 represents unsolvable cases where fail on both the counterfactual pair, 01 represents genuinely learnable instances where succeeds after RL, 10 represents degrade cases, and 11 represents overly-easy instances that is mastered by both models. Accordingly, we define the learnability score of a dataset:

$$L_{SCA} = \alpha_{01} p_{01} + \alpha_{11} p_{11} + \alpha_{10} p_{10} + \alpha_{00} p_{00}. \quad (1)$$

where p denotes the proportion of instances assigned to behavioral category, and α represents the corresponding learnability weight for that category.

3.2 RLVR Dataset Quality Scoring

Grounded in the two complementary perspectives of **Static Quality** and **Dynamic Utility**, whose detailed motivation and design rationale are provided in Appendix C.1, we propose a three-dimensional quantitative metric that forms a composite quality score Q for an RLVR dataset \mathcal{D} , which can be

used to predict RLVR training effectiveness. Full coefficient values are listed in Appendix C.5.

S_1 : Static Data Quality. S_1 aggregates three static sub-scores: the verifiability score S_{1a} , the learnability score S_{1b} , and the contamination robustness score S_{1c} . S_{1a} rewards datasets whose answers are unambiguous and consistently aligned across sources, while penalizing MCQ-heavy data and problems that appear excessively across datasets:

$$S_{1a} = \alpha_{con} R_{con} + \alpha_{mcq} (1 - \beta_{mcq} R_{mcq}) + \alpha_{reuse} P_{reuse}, \quad (2)$$

where R_{con} denotes the fraction of prompts with consistent answers across all occurrences, R_{mcq} is the fraction of MCQs in the dataset, and P_{reuse} is a discount factor that penalizes excessively reused problems across datasets.

S_{1b} is derived from the SCA-annotated learnability score L_{SCA} and augmented with a diversity bonus ε_{div} based on normalized entropy:

$$S_{1b} = \sigma(L_{SCA}) + \varepsilon_{div}, \quad (3)$$

where σ is the sigmoid function used to stabilize the score scale.

S_{1c} measures the proportion of samples in the dataset that are free from confirmed evaluation-set leakage, including both exact-match instances and semantically overlapping instances with evaluation benchmarks. S_{1c} is defined as:

$$S_{1c} = 1 - \frac{N_{leak}}{N}, \quad (4)$$

where N_{leak} denotes the number of leaked samples identified through exact or near-duplicate matching, and N is the total number of samples in the dataset.

S_1 is then computed as a weighted combination:

$$S_1 = w_{1a} \cdot S_{1a} + w_{1b} \cdot S_{1b} + w_{1c} \cdot S_{1c}. \quad (5)$$

S_2 : Sampling Efficiency Gain. S_2 measures improvements in sampling efficiency, reflected by Mean@ N . Since empirical RLVR gains may exhibit different levels of reliability across model scales, we adopt a *scale-adaptive* formulation that combines empirical performance gains with SCA-based learnability attribution L_{SCA} :

$$S_2(\mathcal{D}; M) = \lambda(M) \cdot \widetilde{\Delta\text{Mean@4}} + (1 - \lambda(M)) \cdot L_{SCA}, \quad (6)$$

where $\widetilde{\Delta\text{Mean@4}}$ denotes the normalized Mean@4 improvement on Math500, which serves as both the validation benchmark and a proxy for RLVR learning effectiveness, and $\lambda(M)$ is a scale-dependent interpolation weight determined by the model scale M .

S_3 : Capability Boundary Expansion. S_3 measures improvements in Pass@ N , thereby capturing capability boundary expansion. Similar to S_2 , we combine empirical gains with L_{SCA} :

$$S_3(\mathcal{D}; M) = \lambda(M) \cdot \widetilde{\Delta\text{Pass@4}} + (1 - \lambda(M)) \cdot L_{SCA}, \quad (7)$$

where $\widetilde{\Delta\text{Pass@4}}$ denotes the normalized Pass@4 improvement on Math500.

Composite RLVR Dataset Quality Score. The three dimensions are combined into a single score:

$$Q(\mathcal{D}; M) = w_1(M) \cdot S_1 + w_2(M) \cdot S_2 + w_3(M) \cdot S_3. \quad (8)$$

All scale-dependent weights and coefficients follow $f(M) = a + b \cdot \log_{10}(M/1B)$, allowing the scoring preference to transition smoothly across model scales without discrete thresholds.

Intuitively, larger models place greater emphasis on dynamic utility (e.g., capability boundary expansion and sampling efficiency), while smaller models rely more heavily on static data quality and learnability signals.

4 Experiments

4.1 Experimental Setup

Dataset. Based on the results in Section §2.2, we select DeepScaleR (Luo et al., 2025), OpenR1-Math-220k (Open-R1, 2025), DeepMath-103k (He et al., 2025b), DAPO-Math-17k (Yu et al., 2025), and Skywork-OR1-RL-Data (He et al., 2025a) for evaluation, as these datasets exhibit particularly

representative and distinctive compositional patterns. Additionally, we construct a modified variant named DAPO++, in which leaked instances identified in the original DAPO are removed and replaced with randomly selected non-MCQ and SCA-annotated learnable instances from the *stack exchange* atomic source uncovered by ATLAS, which were rarely inherited by subsequent RLVR datasets.

Implementation Details. The complete set of hyperparameters used in our training and details of the evaluation are provided in Appendix C.2. We use *Qwen3-1.7B-Base* and *Qwen3-8B-Base* (Yang et al., 2025) as the base models and employ GRPO (Shao et al., 2024) as our RL algorithm. We evaluate on eight widely used mathematical reasoning benchmarks: **AMC23** (Zhang and Math-AI, 2023), **AIME24** (Zhang and Math-AI, 2024), **AIME25** (Zhang and Math-AI, 2025), **AMO** (An et al., 2025b), **Minerva** (Lewkowycz et al., 2022), **Olympiad** (He et al., 2024), **HLE** (Phan et al., 2026), and **MATH-500** (Hendrycks et al., 2021)¹. To assess generalization beyond math reasoning, we further test on general reasoning benchmarks **GPQA-Diamond** (Rein et al., 2023), with multiple-choice options shuffled to prevent contamination. For the AMC23, AIME24, AIME25, and AMO benchmark, which have relatively small test sets, we report *Mean@32* (for *Pass@1*), while for the other benchmarks we report *Mean@4*.

Reference Dataset Ranking. Since the relative performance of RLVR datasets varies across model scales, there is no natural ground-truth ranking for dataset quality. To provide a unified reference for evaluating our proposed benchmarking metrics, we construct a reference dataset ranking using *Std-weighted Rank aggregation* (SRank), where rankings from model scales with larger cross-dataset performance variance receive higher weights due to their stronger discriminative power. To account for the discriminative strength of each model scale, we weight each ranking by the cross-dataset standard deviation under that scale:

$$w_m = \frac{\sigma_m}{\sum_{m'} \sigma_{m'}}, \quad (9)$$

where σ_m is the standard deviation of Average* scores across datasets for model scale m . The final

¹Since *Math500* is used as the validation set for checkpoint selection in all experiments, we exclude it from the average score computation and denote the resulting metric as average*.

aggregated rank score for dataset D is defined as:

$$SRank(D) = \sum_m w_m \cdot \text{rank}_m(D). \quad (10)$$

4.2 Experimental Results

Reasoning Performance. Based on the leakage analysis in Section §2.2, we construct decontaminated versions of five selected representative datasets, train corresponding RLVR checkpoints on them, and evaluate their performance on both mathematical reasoning benchmarks (Table 1) and general reasoning tasks (Table 10).

We first observe substantial differences in dataset discriminability across model scales. Specifically, the performance gaps among datasets are relatively small under the 1.7B setting (std.=0.59), whereas the 8B setting exhibits much clearer dataset separation (std.=2.17). Additionally, while DAPO++ consistently achieves the best overall performance across both model scales, the second best-performing dataset is not consistent across scales: DeepMath-103K performs stronger under the 1.7B setting, whereas DAPO performs better among the remaining baselines under the 8B setting. Therefore, based on our proposed SRank metric (Table 2), we obtain the unified reference ranking of RLVR datasets as follows: DAPO++ (ours) > DAPO > DeepScaleR > DeepMath > Skywork > OpenR1.

Benchmark Result. Using the quality scoring framework proposed in Section §3.2, along with the corresponding SCA-based *Mean@N* and *Pass@N* results reported in Appendix C.4, we obtain the quality scores shown in Table 3. First, our quality scores exhibit strong correlation with the averaged mathematical reasoning performance. In particular, the Spearman correlations between the Q scores and Average* performance reach 0.60 and 0.94 under the 1.7B and 8B settings, respectively, indicating that our scoring framework effectively captures dataset utility trends. Moreover, compared with the reference ranking constructed by SRank, our scoring method remains highly consistent with the more discriminative 8B ranking ($\rho = 0.93$), while moderately smoothing the noisier 1.7B ranking ($\rho = 0.54$). These results collectively demonstrate the validity and robustness of our proposed scoring framework.

Ablation Study. We conduct ablation studies on the two key factors of high-quality RLVR data proposed in Static Quality, namely *Verifiability* and *Contamination*.

As shown in Table 4, converting MCQ data into open-ended questions consistently improves the Average* score. This suggests that, compared to multiple-choice formats, open-ended questions provide more reliable and consistent supervision signals, thereby improving reward verifiability and learnability during RLVR training. The results validate the importance of high *Verifiability* in constructing effective RLVR datasets.

Furthermore, as shown in Table 5, removing contaminated data does not hurt performance; instead, it leads to overall improvements, with the largest gains observed on challenging benchmarks such as AIME. This indicates that leaked data are not necessarily useful difficult data, but may instead contain high-noise or low-learnability signals. Moreover, performance improvements obtained by existing methods on contaminated datasets do not necessarily imply genuine reasoning capability, but may partially stem from memorizing leaked evaluation instances themselves. These findings further underscore the significance of our systematic data collection and lineage tracing framework, which makes large-scale global decontamination across RLVR corpora possible, thereby enabling the construction of cleaner, more reliable, and contamination-controlled training datasets.

5 Conclusion

In this work, we propose *ATLAS*, a lineage-aware atomic-source tracing framework for large-scale provenance analysis in RLVR datasets. Using *ATLAS*, we uncover the hidden composition of widely used RLVR datasets, revealing substantial overlap in their upstream sources and significant contamination risks. Guided by these findings, we further curate a new RLVR dataset, DAPO++. Beyond provenance tracing, we introduce SCA, a source-aware attribution framework for RLVR dataset benchmarking and quality estimation, together with a composite dataset quality score Q for predicting downstream RLVR effectiveness. Overall, our work provides a roadmap for RLVR dataset construction, benchmarking, and selection, laying the foundation for future RLVR research.

Limitations

Although *ATLAS* traces over one million RLVR instances back to their atomic sources, the tracing process still relies heavily on manual curation and human audit. In particular, many early math-

Source	Mean@4				Mean@32				Average*
	Math500*	Minerva	Olympiad	HLE	AMC23	AIME24	AIME25	AMO	
Qwen3-1.7B-Base	48.4	15.3	17.6	5.9	28.2	4.7	2.3	1.3	10.8
↪ DeepScaleR	58.1	23.3	23.7	6.3	34.5	6.3	7.6	1.0	14.7
↪ DeepMath-103K	57.9	26.5	23.1	8.4	35.4	8.4	3.1	3.2	15.4
↪ OpenR1-Math-220k	58.9	23.1	24.0	4.7	31.6	6.9	6.3	1.4	14.0
↪ DAPO-Math-17k	58.5	22.6	22.9	5.9	39.5	7.0	5.9	1.3	15.0
↪ Skywork-OR1-RL-Data	58.8	22.8	24.7	5.1	40.9	5.8	4.6	2.0	15.1
↪ DAPO++ (ours)	60.0	21.9	24.9	6.8	41.9	9.4	3.3	1.7	15.7
Qwen3-8B-Base	61.6	25.6	27.9	5.7	48.6	10.4	10.5	1.8	18.6
↪ DeepScaleR	75.9	34.7	38.8	4.5	61.6	23.4	17.1	2.9	26.1
↪ DeepMath-103K	73.4	31.9	39.2	4.5	62.7	17.1	16.7	3.7	25.1
↪ OpenR1-Math-220k	73.1	35.7	37.0	3.9	63.2	16.5	15.4	3.3	25.0
↪ DAPO-Math-17k	77.8	36.7	43.0	4.1	69.8	27.9	21.5	2.4	29.3
↪ Skywork-OR1-RL-Data	73.2	34.5	37.8	3.1	64.1	17.3	15.8	2.8	25.1
↪ DAPO++ (ours)	77.7	37.1	43.5	4.7	69.3	25.9	22.6	3.9	29.6

Table 1: RLVR results on the *decontaminated versions of datasets* after removing leaked or test-set-related instances.

Dataset	Qwen3-1.7B Avg. (Rank)	Qwen3-8B Avg. (Rank)	SRank↓ Score (Rank)
DAPO++	15.7 (1)	29.6 (1)	1.00 (1)
DAPO	15.0 (4)	29.3 (2)	2.43 (2)
DeepScaleR	14.7 (5)	26.1 (3)	3.43 (3)
DeepMath	15.4 (2)	25.1 (4)	3.57 (4)
Skywork	15.1 (3)	25.1 (4)	3.79 (5)
OpenR1	14.0 (6)	25.0 (6)	6.00 (6)

Table 2: Reference dataset ranking constructed using SRank. The final score of SRank places DAPO as the top-ranked RLVR dataset.

ematical reasoning datasets exhibit severe nested reuse and ambiguous provenance chains, requiring careful inspection of original papers and dataset documentation to disentangle hidden dependencies (e.g., draw, and asdiv). Due to the substantial manual effort required for reliable attribution, as well as the incomplete availability and gradual loss of older papers and dataset resources, our current tracing only recovers several lineage branches back to approximately 2014-era datasets (e.g., AddSub and SimulEq). Therefore, older data sources remain to be incorporated in future work.

Ethics Statement

Use of AI Assistants. We have employed ChatGPT as a writing assistant, primarily for polishing the text after the initial composition. We certify that any use of AI tools, including ChatGPT, was strictly limited to linguistic refinement such as improving grammar, clarity, and style. All substantive ideas, analyses, and arguments presented in this work originate from the authors or from properly

Dataset	S1	S2	S3	Q↑ (Rank)
Qwen3-1.7B-Base				
DeepScaleR	0.901	0.685	0.616	0.804 (5)
DeepMath	0.980	0.795	0.720	0.895 (2)
OpenR1	0.906	0.511	0.443	0.738 (6)
DAPO	0.969	0.836	0.788	0.909 (1)
Skywork	0.944	0.796	0.740	0.876 (4)
DAPO++ (ours)	0.967	0.728	0.772	0.878 (3)
Pearson r	+0.81	+0.75	+0.89	+0.85
Spearman ρ	+0.66	+0.43	+0.60	+0.60
Qwen3-8B-Base				
DeepScaleR	0.811	0.678	0.442	0.654 (2)
DeepMath	0.890	0.569	0.289	0.598 (3)
OpenR1	0.825	0.539	0.212	0.541 (5)
DAPO	0.897	0.772	0.539	0.746 (2)
Skywork	0.857	0.561	0.206	0.558 (4)
DAPO++ (ours)	0.929	0.778	0.524	0.754 (1)
Pearson r	+0.70	+0.96	+0.91	+0.96
Spearman ρ	+0.60	+0.94	+0.77	+0.94

S_1 : Static Data Quality, S_2 : Sampling Efficiency, S_3 : Capability Boundary Expansion, and Q : Overall Quality Score.

Table 3: Multi-dimensional quality scores. Pearson r and Spearman ρ are computed between the Q scores and Average* results in Table 1.

cited prior research.

Computational Budget. All our experiments are conducted on a machine with CentOS 8, 384 AMD® EPYC™ 9K84 96-Core Processor CPUs and 2.2TiB memory. We use 8× NVIDIA H20 GPUs for all experiments. GRPO training takes approximately 3 and 7 days per experiment for the 1.7B and 8B models, respectively.

Reproducibility. Our work is reproducible because we have provided our source code and imple-

Source	Math500*	Minerva	Olympiad	HLE	AMC23	AIME24	AIME25	AMO	Average*
<i>Qwen3-1.7B-Base</i>	48.4	15.3	17.6	5.9	28.2	4.7	2.3	1.3	10.8
olympiads	57.8	22.3	23.1	6.1	35.1	5.3	5.2	2.1	14.2
↔ w/o mcq	59.0	24.1	23.2	5.5	36.2	9.4	3.3	1.8	14.8
amc_aim	58.7	23.0	23.6	7.0	36.8	8.4	4.3	1.9	15.0
↔ w/o mcq	59.1	21.5	23.3	5.5	46.0	10.4	5.7	2.5	16.4

Table 4: Mean@N results for MCQ ablation.

Model	Dataset	Math500*	Minerva	Olympiad	HLE	AMC23	AIME24	AIME25	AMO	Average*
<i>Qwen3-1.7B</i>	DeepScaleR	58.7	22.3	23.9	5.5	33.7	6.3	4.3	2.8	14.1
	↔ Decontam.	58.1	23.3	23.7	6.3	34.5	6.3	7.6	1.0	14.7
<i>Base</i>	DAPO-Math-17k	59.7	22.2	24.0	6.8	37.1	5.3	5.0	1.9	14.6
	↔ Decontam.	58.5	22.6	22.9	5.9	39.5	7.0	5.9	1.3	15.0
<i>Qwen3-8B</i>	DeepScaleR	73.0	33.9	37.0	3.5	62.7	16.9	14.2	2.8	24.4
	↔ Decontam.	75.9	34.7	38.8	4.5	61.6	23.4	17.1	2.9	26.1
<i>Base</i>	DAPO-Math-17k	79.4	36.8	43.6	4.1	68.8	28.1	21.7	2.6	29.4
	↔ Decontam.	77.7	35.7	43.7	4.3	69.6	28.4	22.7	2.8	29.6

Table 5: Mean@N results for decontamination ablation across mathematical reasoning benchmarks.

mentation details.

Scientific Artifacts. The scientific artifacts we use are shown in Table 6, with links provided. License information can be found at the corresponding links. All existing artifacts were used in a manner consistent with their intended purpose, namely RLVR training and evaluation. All datasets used and constructed in this work are derived from publicly available open-source data; therefore, data consent considerations are not applicable to this work.

Clarification on Human Subjects. The data annotation and verification procedures in this work were conducted entirely by the authors through case-by-case manual inspection. **No** crowdworkers, external annotators, or paid labeling services were recruited during the annotation process. Therefore, considerations regarding crowdworker recruitment and compensation are not applicable to this work.

Potential Risks. To the best of our knowledge, there are no potential risks concerning our work.

References

- Alon Albalak, Duy Phung, Nathan Lile, Rafael Rafailov, Kanishk Gandhi, Louis Castricato, Anikait Singh, Chase Blagden, Violet Xiang, Dakota Mahan, and Nick Haber. 2025. [Big-math: A large-scale, high-quality math dataset for reinforcement learning in language models](#). *Preprint*, arXiv:2502.17387.
- Chenxin An, Zhihui Xie, Xiaonan Li, Lei Li, Jun Zhang, Shansan Gong, Ming Zhong, Jingjing Xu, Xipeng Qiu, Mingxuan Wang, and Lingpeng Kong. 2025a. [Polaris: A post-training recipe for scaling reinforcement learning on advanced reasoning models](#).
- Shengnan An, Xunliang Cai, Xuezhi Cao, Xiaoyu Li, Yehao Lin, Junlin Liu, Xinxuan Lv, Dan Ma, Xuanlin Wang, Ziwen Wang, and Shuang Zhou. 2025b. [Amo-bench: Large language models still struggle in high school math competitions](#). *Preprint*, arXiv:2510.26768.
- Andrew Brooks. 2025. What is synthetic data and why it matters now. <https://www.linkedin.com/pulse/what-synthetic-data-why-matters-now-andrew-brooks-8hbze/>. LinkedIn article, accessed May 8, 2026.
- Yang Chen, Zhuolin Yang, Zihan Liu, Chankyu Lee, Peng Xu, Mohammad Shoeybi, Bryan Catanzaro, and Wei Ping. 2025a. [Acereason-nemotron: Advancing math and code reasoning through reinforcement learning](#). *Preprint*, arXiv:2505.16400.
- Zhipeng Chen, Yingqian Min, Beichen Zhang, Jie Chen, Jinhao Jiang, Daixuan Cheng, Wayne Xin Zhao, Zheng Liu, Xu Miao, Yang Lu, Lei Fang, Zhongyuan Wang, and Ji-Rong Wen. 2025b. [An empirical study on eliciting and improving rl-like reasoning models](#). *Preprint*, arXiv:2503.04548.
- Yuxing Cheng, Yi Chang, and Yuan Wu. 2025. [A survey on data contamination for large language models](#). *Preprint*, arXiv:2502.14425.
- Karl Cobbe, Vineet Kosaraju, Mohammad Bavarian, Mark Chen, Heewoo Jun, Lukasz Kaiser, Matthias Plappert, Jerry Tworek, Jacob Hilton, Reiichiro

- Nakano, Christopher Hesse, and John Schulman. 2021. [Training verifiers to solve math word problems](#). *Preprint*, arXiv:2110.14168.
- Ganqu Cui, Lifan Yuan, Zefan Wang, Hanbin Wang, Wendi Li, Bingxiang He, Yuchen Fan, Tianyu Yu, Qixin Xu, Weize Chen, and 1 others. 2025. [Process reinforcement through implicit rewards](#). *arXiv preprint arXiv:2502.01456*.
- Meng Fang, Xiangpeng Wan, Fei Lu, Fei Xing, and Kai Zou. 2025. [Mathodyssey: Benchmarking mathematical problem-solving skills in large language models using odyssey math data](#). *Scientific Data*, 12(1):1392.
- Yujuan Fu, Ozlem Uzuner, Meliha Yetisgen, and Fei Xia. 2025. [Does data contamination detection work \(well\) for LLMs? a survey and evaluation on detection assumptions](#). In *Findings of the Association for Computational Linguistics: NAACL 2025*, pages 5250–5271, Albuquerque, New Mexico. Association for Computational Linguistics.
- Bofei Gao, Feifan Song, Zhe Yang, Zefan Cai, Yibo Miao, Qingxiu Dong, Lei Li, Chenghao Ma, Liang Chen, Runxin Xu, Zhengyang Tang, Benyou Wang, Daoguang Zan, Shanghaoran Quan, Ge Zhang, Lei Sha, Yichang Zhang, Xuancheng Ren, Tianyu Liu, and Baobao Chang. 2024. [Omni-math: A universal olympiad level mathematic benchmark for large language models](#). *Preprint*, arXiv:2410.07985.
- Amirata Ghorbani and James Zou. 2019. [Data shapley: Equitable valuation of data for machine learning](#). In *Proceedings of the 36th International Conference on Machine Learning*, volume 97 of *Proceedings of Machine Learning Research*, pages 2242–2251. PMLR.
- Chaoqun He, Renjie Luo, Yuzhuo Bai, Shengding Hu, Zhen Leng Thai, Junhao Shen, Jinyi Hu, Xu Han, Yujie Huang, Yuxiang Zhang, Jie Liu, Lei Qi, Zhiyuan Liu, and Maosong Sun. 2024. [Olympiadbench: A challenging benchmark for promoting agi with olympiad-level bilingual multimodal scientific problems](#). *Preprint*, arXiv:2402.14008.
- Jujie He, Jiakai Liu, Chris Yuhao Liu, Rui Yan, Chaojie Wang, Peng Cheng, Xiaoyu Zhang, Fuxiang Zhang, Jiacheng Xu, Wei Shen, Siyuan Li, Liang Zeng, Tianwen Wei, Cheng Cheng, Bo An, Yang Liu, and Yahui Zhou. 2025a. [Skywork open reasoner 1 technical report](#). *Preprint*, arXiv:2505.22312.
- Zhiwei He, Tian Liang, Jiahao Xu, Qiuzhi Liu, Xingyu Chen, Yue Wang, Linfeng Song, Dian Yu, Zhenwen Liang, Wenxuan Wang, Zhuosheng Zhang, Rui Wang, Zhaopeng Tu, Haitao Mi, and Dong Yu. 2025b. [Deepmath-103k: A large-scale, challenging, decontaminated, and verifiable mathematical dataset for advancing reasoning](#). *Preprint*, arXiv:2504.11456.
- Dan Hendrycks, Collin Burns, Saurav Kadavath, Akul Arora, Steven Basart, Eric Tang, Dawn Song, and Jacob Steinhardt. 2021. [Measuring mathematical problem solving with the math dataset](#). *Preprint*, arXiv:2103.03874.
- Richard Hohensinner, Belgin Mutlu, Inti Gabriel Mendoza Estrada, Matej Vukovic, Simone Kopeinik, and Roman Kern. 2026. [Tracing the data trail: A survey of data provenance, transparency and traceability in llms](#). *Preprint*, arXiv:2601.14311.
- Jingcheng Hu, Yinmin Zhang, Qi Han, Daxin Jiang, Xiangyu Zhang, and Heung-Yeung Shum. 2025a. [Open-reasoner-zero: An open source approach to scaling up reinforcement learning on the base model](#). *Preprint*, arXiv:2503.24290.
- Yuzheng Hu, Fan Wu, Haotian Ye, David Forsyth, James Zou, Nan Jiang, Jiaqi W. Ma, and Han Zhao. 2025b. [A snapshot of influence: A local data attribution framework for online reinforcement learning](#). *Preprint*, arXiv:2505.19281.
- inclusionAI. 2025. [Areal-boba-data](#).
- Pang Wei Koh and Percy Liang. 2020. [Understanding black-box predictions via influence functions](#). *Preprint*, arXiv:1703.04730.
- Aitor Lewkowycz, Anders Andreassen, David Dohan, Ethan Dyer, Henryk Michalewski, Vinay Ramasesh, Ambrose Slone, Cem Anil, Imanol Schlag, Theo Gutman-Solo, Yuhuai Wu, Behnam Neyshabur, Guy Gur-Ari, and Vedant Misra. 2022. [Solving quantitative reasoning problems with language models](#). In *Advances in Neural Information Processing Systems*, volume 35, pages 3843–3857. Curran Associates, Inc.
- Jia Li, Edward Beeching, Lewis Tunstall, Ben Lipkin, Roman Soletskyi, Shengyi Costa Huang, Kashif Rasul, Longhui Yu, Albert Jiang, Ziju Shen, Zihan Qin, Bin Dong, Li Zhou, Yann Fleureau, Guillaume Lample, and Stanislas Polu. 2024. [Numinamath](#). [<https://huggingface.co/datasets/AI-MO/NuminaMath-CoT>](https://github.com/project-numina/aimo-progress-prize/blob/main/report/numina_dataset.pdf).
- Michael Luo, Sijun Tan, Justin Wong, Xiaoxiang Shi, William Tang, Manan Roongta, Colin Cai, Jeffrey Luo, Tianjun Zhang, Erran Li, Raluca Ada Popa, and Ion Stoica. 2025. [DeepScaler: Surpassing o1-preview with a 1.5b model by scaling rl](#). <https://pretty-radio-b75.notion.site/DeepScaleR-Surpassing-O1-Preview-with-a-1-5B-Model-by-Scaling-RL-19681902c1468005bed8ca303013a4e2>. Notion Blog.
- Thang Luong, Dawsen Hwang, Hoang H Nguyen, Golnaz Ghiasi, Yuri Chervonyi, Insuk Seo, Junsu Kim, Garrett Bingham, Jonathan Lee, Swaroop Mishra, Alex Zhai, Huiyi Hu, Henryk Michalewski, Jimin Kim, Jeonghyun Ahn, Junhwi Bae, Xingyou Song, Trieu Hoang Trinh, Quoc V Le, and Junehyuk Jung. 2025. [Towards robust mathematical reasoning](#). In *Proceedings of the 2025 Conference on Empirical*

- Methods in Natural Language Processing*, pages 35418–35442, Suzhou, China. Association for Computational Linguistics.
- Yingqian Min, Zhipeng Chen, Jinhao Jiang, Jie Chen, Jia Deng, Yiwen Hu, Yiru Tang, Jiapeng Wang, Xiaoxue Cheng, Huatong Song, Wayne Xin Zhao, Zheng Liu, Zhongyuan Wang, and Ji-Rong Wen. 2024. [Imitate, explore, and self-improve: A reproduction report on slow-thinking reasoning systems](#). *Preprint*, arXiv:2412.09413.
- Swaroop Mishra, Matthew Finlayson, Pan Lu, Leonard Tang, Sean Welleck, Chitta Baral, Tanmay Rajpurohit, Oyvind Taffjord, Ashish Sabharwal, Peter Clark, and Ashwin Kalyan. 2022. [LILA: A unified benchmark for mathematical reasoning](#). In *Proceedings of the 2022 Conference on Empirical Methods in Natural Language Processing*, pages 5807–5832, Abu Dhabi, United Arab Emirates. Association for Computational Linguistics.
- Open-R1. 2025. [Openr1-math-220k](#).
- Long Phan, Alice Gatti, Nathaniel Li, Adam Khoja, Ryan Kim, Richard Ren, Jason Hausenloy, Oliver Zhang, Mantas Mazeika, Dan Hendrycks, Ziwen Han, Josephina Hu, Hugh Zhang, Chen Bo Calvin Zhang, Mohamed Shaaban, and et al. 2026. [A benchmark of expert-level academic questions to assess ai capabilities](#). *Nature*, 649(8099):1139–1146.
- Qi Qian, Chengsong Huang, Jingwen Xu, Changze Lv, Muling Wu, Wenhao Liu, Xiaohua Wang, Zhenghua Wang, Zisu Huang, Muzhao Tian, Jianhan Xu, Kun Hu, He-Da Wang, Yao Hu, Xuanjing Huang, and Xiaoqing Zheng. 2026. [Benchmark²: Systematic evaluation of llm benchmarks](#). *Preprint*, arXiv:2601.03986.
- Nils Reimers and Iryna Gurevych. 2019. [Sentence-BERT: Sentence embeddings using Siamese BERT-networks](#). In *Proceedings of the 2019 Conference on Empirical Methods in Natural Language Processing and the 9th International Joint Conference on Natural Language Processing (EMNLP-IJCNLP)*, pages 3982–3992, Hong Kong, China. Association for Computational Linguistics.
- David Rein, Betty Li Hou, Asa Cooper Stickland, Jackson Petty, Richard Yuanzhe Pang, Julien Dirani, Julian Michael, and Samuel R. Bowman. 2023. [Gpqa: A graduate-level google-proof q&a benchmark](#). *Preprint*, arXiv:2311.12022.
- ByteDance Seed. 2025. [Seed1.5-thinking: Advancing superb reasoning models with reinforcement learning](#). *Preprint*, arXiv:2504.13914.
- Zhihong Shao, Peiyi Wang, Qihao Zhu, Runxin Xu, Junxiao Song, Xiao Bi, Haowei Zhang, Mingchuan Zhang, Y. K. Li, Y. Wu, and Daya Guo. 2024. [Deepseekmath: Pushing the limits of mathematical reasoning in open language models](#). *Preprint*, arXiv:2402.03300.
- Guangming Sheng, Chi Zhang, Zilingfeng Ye, Xibin Wu, Wang Zhang, Ru Zhang, Yanghua Peng, Haibin Lin, and Chuan Wu. 2025. [Hybridflow: A flexible and efficient rlhf framework](#). In *Proceedings of the Twentieth European Conference on Computer Systems*, EuroSys '25, page 1279–1297, New York, NY, USA. Association for Computing Machinery.
- Zhenpeng Su, Leiyu Pan, Xue Bai, Dening Liu, Guanting Dong, Jiaming Huang, Wenping Hu, Fuzheng Zhang, Kun Gai, and Guorui Zhou. 2026. [Klear-reasoner: Advancing reasoning capability via gradient-preserving clipping policy optimization](#). *Preprint*, arXiv:2508.07629.
- Jianhao Yan, Yafu Li, Zican Hu, Zhi Wang, Ganqu Cui, Xiaoye Qu, Yu Cheng, and Yue Zhang. 2025. [Learning to reason under off-policy guidance](#). *Preprint*, arXiv:2504.14945.
- An Yang, Anfeng Li, Baosong Yang, Beichen Zhang, Binyuan Hui, Bo Zheng, Bowen Yu, Chang Gao, Chengen Huang, Chenxu Lv, Chujie Zheng, Dayiheng Liu, Fan Zhou, Fei Huang, Feng Hu, Hao Ge, Haoran Wei, Huan Lin, Jialong Tang, and 41 others. 2025. [Qwen3 technical report](#). *Preprint*, arXiv:2505.09388.
- Qiyang Yu, Zheng Zhang, Ruofei Zhu, Yufeng Yuan, Xiaochen Zuo, Yu Yue, Weinan Dai, Tiantian Fan, Gaohong Liu, Lingjun Liu, Xin Liu, Haibin Lin, Zhiqi Lin, Bole Ma, Guangming Sheng, Yuxuan Tong, Chi Zhang, Mofan Zhang, Wang Zhang, and 16 others. 2025. [Dapo: An open-source llm reinforcement learning system at scale](#). *Preprint*, arXiv:2503.14476.
- Albert S. Yue, Lovish Madaan, Ted Moskowitz, DJ Strouse, and Aaditya K. Singh. 2024. [Harp: A challenging human-annotated math reasoning benchmark](#). *Preprint*, arXiv:2412.08819.
- Yifan Zhang and Team Math-AI. 2023. [American mathematics competitions](#).
- Yifan Zhang and Team Math-AI. 2024. [American invitational mathematics examination \(aime\) 2024](#).
- Yifan Zhang and Team Math-AI. 2025. [American invitational mathematics examination \(aime\) 2025](#).
- Xinyu Zhou, Boyu Zhu, Haotian Zhang, Huiming Wang, and Zhijiang Guo. 2026. [Efficient rlvr training via weighted mutual information data selection](#). *Preprint*, arXiv:2603.01907.
- Longyuan Zhu, Hairan Hua, Linlin Miao, and Bing Zhao. 2026. [Benchmark health index: A systematic framework for benchmarking the benchmarks of llms](#). *Preprint*, arXiv:2602.11674.

A Details of Data Lineage Tracing

A.1 Collected RLVR Datasets and Traced Atomic Sources

Based on the limited data provenance described in the HuggingFace repositories, blogs or associated papers of these RLVR datasets, we conduct an iterative and labor-intensive data lineage analysis to identify 5 core data sources. Among them, 3 are large-scale aggregated data that compile substantial amounts of prior datasets, while the remaining 2 are more atomic sources, a non-trivial portion of whose contents has been reused in subsequent datasets without explicit attribution. Detailed statistics of all datasets, including their HuggingFace ids, corresponding papers, and dataset sizes, are provided in Table 6. Meanwhile, Table 7 summarizes the atomic sources traced by ATLAS. The problem-type labels are manually annotated through case inspection and careful examination of the associated papers and dataset construction documentation.

A.2 ATLAS Pipeline

ATLAS is composed of three stages, and the overall tracing procedure is summarized in Algorithm 1.

A.3 RLVR Dataset Provenance

Figure 5 further reveals the specific RLVR datasets in which these atomic data sources were first introduced. Although many datasets exhibit substantial atomic source overlap, particularly with the NuminaMath-CoT and NuminaMath-1.5 series (Li et al., 2024), we still observe considerable heterogeneity in the relative source proportions across datasets. We further visualize the compositional relationships among RLVR datasets using Bokeh plots, where the detailed views for each dataset are provided in Figure 6.

B Details of Leakage Analysis

B.1 Source Leakage

Figure 7 presents the benchmark leakage statistics of major source datasets measured by semantic overlap. We primarily report high-risk leakage cases with semantic similarity scores exceeding 90%, while noting that a small number of potentially leaked cases may remain in the 80% similarity range.

Algorithm 1 Iterative Data Lineage Tracing

Input: Initial dataset pool \mathcal{P} sorted by time; thresholds τ, δ
Output: Lineage dictionary $\mathcal{L}[h]$
Initialize $\mathcal{L} \leftarrow \emptyset$, unmatched set $\mathcal{U} \leftarrow \emptyset$
repeat
 Stage 0: Data Collection and Canonicalization
 collect candidate datasets \mathcal{D}_{new}
 for each dataset $D' \in \mathcal{D}_{\text{new}}$ **do**
 canonicalize each instance into $d = (h, p, q, a, s, \text{id}, t)$ via canonicalization and SHA1 hashing
 add processed dataset D to \mathcal{P}
 end for
 Stage 1: Temporal Index Matching
 for each instance $d = (h, p, q, a, s, \text{id}, t) \in \mathcal{P}$ in chronological order **do**
 if $h \in \mathcal{L}$ **then**
 append (id, t, a, s) to $\mathcal{O}[h]$
 else
 create $\mathcal{L}[h]$ and initialize $\mathcal{O}[h]$ with (id, t, a, s)
 end if
 end for
 Stage 2: Similarity-Based Matching
 manually inspect unmatched records and apply rule set R to construct \mathcal{U}
 for each instance $d \in \mathcal{U}$ **do**
 find nearest prompt group $p \in \mathcal{L}[h]$ by cosine similarity
 if $\cos(h, h') \geq \delta$ **then**
 merge $\mathcal{O}[h]$ into $\mathcal{O}[h']$, remove key h from \mathcal{L} , remove h from \mathcal{U}
 end if
 end for
 Stage 3: Iterative Source Recovery
 if $|\mathcal{U}| > \tau$ **then**
 manually identify candidate datasets, add \mathcal{D}_{new} to \mathcal{P}
 return Stage 1 and Stage 2
 end if
until $|\mathcal{U}| \leq \tau$
return $\mathcal{L}[h]$

Dataset	Date	Huggingface	Length	Link
Data Source (Data Source Collection† / Atomic Source)				
Lila† (Mishra et al., 2022)	2022.10.11	allenai/lila	317k	🔗 📄
NuminaMath-CoT† (Li et al., 2024)	2024.07.22	AI-MO/NuminaMath-CoT	859k	🔗 📄
Still-1 (Min et al., 2024)	2024.12.12	RUC-AIBOX/long_form_thought_data_5k	4.92k	🔗 📄
Olympiads-Ref (Li et al., 2024)	2024.12.20	AI-MO/olympiads-ref-base	13.1k	🔗 -
NuminaMath-1.5† (Li et al., 2024)	2025.02.10	AI-MO/NuminaMath-1.5	896k	🔗 -
RLVR Datasets (Curated with Verifiable Rewards)				
Eurus-2-RL-Data (Cui et al., 2025)	2025.02.03	PRIME-RL/Eurus-2-RL-Data	481k	🔗 📄
DeepScaleR (Luo et al., 2025)	2025.02.10	agentic-org/DeepScaleR-Preview-Dataset	40.3k	🔗 📄
DeepMath-103K (He et al., 2025b)	2025.02.15	zwhe99/DeepMath-103K	103k	🔗 📄
OpenR1-Math-220k (Open-R1, 2025)	2025.02.18	open-r1/OpenR1-Math-220k	220k	🔗 -
STILL-3-RL-90K (Chen et al., 2025b)	2025.03.06	RUC-AIBOX/STILL-3-RL-90K	88.1k	🔗 📄
DAPO-Math-17k (Yu et al., 2025)	2025.03.18	BytedTsinghua-SIA/DAPO-Math-17k	17k	🔗 📄
Big-Math (Albalak et al., 2025)	2025.03.25	open-r1/Big-Math-RL-Verified-Processed	216k	🔗 📄
AReal-boba-Data (inclusionAI, 2025)	2025.03.29	inclusionAI/AReal-boba-Data	106k	🔗 📄
ORZ-72k (Hu et al., 2025a)	2025.04.06	Open-Reasoner-Zero/orz_math_72k_collection	72.4k	🔗 📄
AceReason-Math (Chen et al., 2025a)	2025.05.22	nvidia/AceReason-Math	49.6k	🔗 📄
Skywork-OR1-RL-Data (He et al., 2025a)	2025.05.29	Skywork/Skywork-OR1-RL-Data	105k	🔗 📄
Polaris-53K (An et al., 2025a)	2025.06.18	POLARIS-Project/Polaris-Dataset-53K	53.3k	🔗 📄
KlearMathSub-30K (Su et al., 2026)	2025.08.11	Kwai-Klear/KlearReasoner-MathSub-30K	30k	🔗 📄
Mathematical Reasoning Benchmarks (Test Sets)				
MATH-500 (Hendrycks et al., 2021)	2021.03.05	HuggingFaceH4/MATH-500	-	🔗 📄
GSM8K (Cobbe et al., 2021)	2021.10.27	openai/gsm8k	-	🔗 📄
MinervaMath (Lewkowycz et al., 2022)	2022.06.29	math-ai/minervamath	-	🔗 📄
OlympiadBench (He et al., 2024)	2024.02.21	knoveleng/OlympiadBench	-	🔗 📄
MathOdyssey (Fang et al., 2025)	2024.06.26	MathOdyssey/MathOdyssey	-	🔗 📄
Omni-MATH (Gao et al., 2024)	2024.09.14	KbsdJames/Omni-MATH	-	🔗 📄
HARP (Yue et al., 2024)	2024.12.11	HARP (Released only on GitHub)	-	🔗 📄
HLE-Math (Phan et al., 2026)	2025.01.24	cais/hle	-	🔗 📄
BeyondAIME (Seed, 2025)	2025.06.17	ByteDance-Seed/BeyondAIME	-	🔗 📄
AMO-Bench (An et al., 2025b)	2025.10.29	meituan-longcat/AMO-Bench	-	🔗 📄
IMO-AnswerBench (Luong et al., 2025)	2025.11.05	Hwilner/imo-answerbench	-	🔗 📄
AMC23 (Zhang and Math-AI, 2023)	-	math-ai/amc23	-	🔗 -
AIME24 (Zhang and Math-AI, 2024)	-	math-ai/aime24	-	🔗 -
AIME25 (Zhang and Math-AI, 2025)	-	math-ai/aime25	-	🔗 -

Table 6: Data sources, RLVR datasets and test sets used in this work. For competition datasets (AMC23, AIME24, and AIME25), we cite the corresponding HuggingFace dataset pages since these datasets are primarily distributed through HuggingFace.

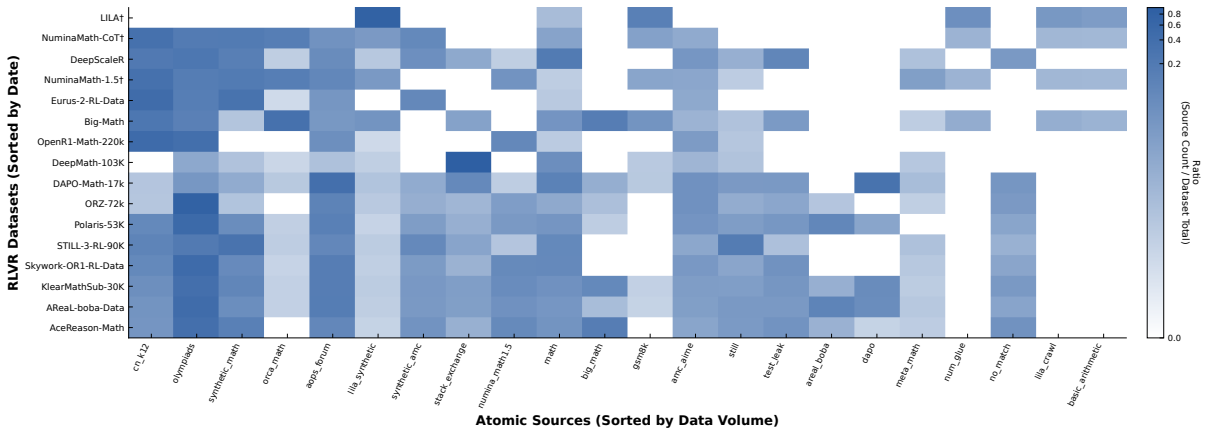


Figure 5: Atomic-source distributions across datasets. Reading each column from top to bottom, the first colored cell denotes the dataset in which the corresponding atomic source was first introduced into the RLVR data ecosystem.

Source Label	Size	Problem Type	Merged Atomic Sources
Non-synthetic / Real-world Data			
cn_k12	342,217	MWP	{cn_k12}
olympiads	296,998	Competition	{olympiads, olympiads_ref}
aops_forum	107,244	Competition (Forum)	{aops_forum}
stack_exchange	97,025	Forum	{deepmath_stack_exchange}
big_math	32,227	Mixed	{big_math_reformulated}
numina_math1.5	26,821	Mixed	{cn_contest, inequalities, number_theory}
still	18,175	Mixed	{still1, still3}
gsm8k	14,869	MWP	{gsm8k}
areal_boba*	14,838	Mixed	{areal_boba, areal_boba_synthetic}
amc_aime	10,265	Competition	{amc_aime, aime19832023}
math	9,877	Competition	{math, math(lila)}
dapo	5,294	Mixed	{dapo}
num_glue	4,925	MWP	{num_glue}
lila_crawl	2,635	MWP	{draw, asdiv}
basic_arithmetic	1,829	MWP	{addsub, simuleq, singleop, singleq, multiarith}
Synthetic / Weakly-Synthetic			
synthetic_math	149,520	Synthetic	{synthetic_math}
orca_math	125,311	Synthetic	{orca_math}
lila_synthetic	86,172	Synthetic	{svamp, mathqa, deepmind_mathematics, amps}
synthetic_amc	83,407	Synthetic	{synthetic_amc}
meta_math	11,011	Synthetic	{meta_math}
Special Handling / Filtered			
test_leak	6,093	Competition	{omni_math, math_odyssey, harp, amc23}
no_match	4,074	Unknown	{N/A}
Total	1,450,827	-	-

Table 7: Source labels and their merged atomic sources. `test_leak` denotes datasets originally proposed as **evaluation benchmarks** without official train/dev/test splits, which may therefore be exposed to potential leakage risks depending on the training protocol. Although a subset (e.g., `areal_boba_synthetic`) may contain weakly synthetic data based on our manual inspection, we conservatively categorize it as real-world data in this work.

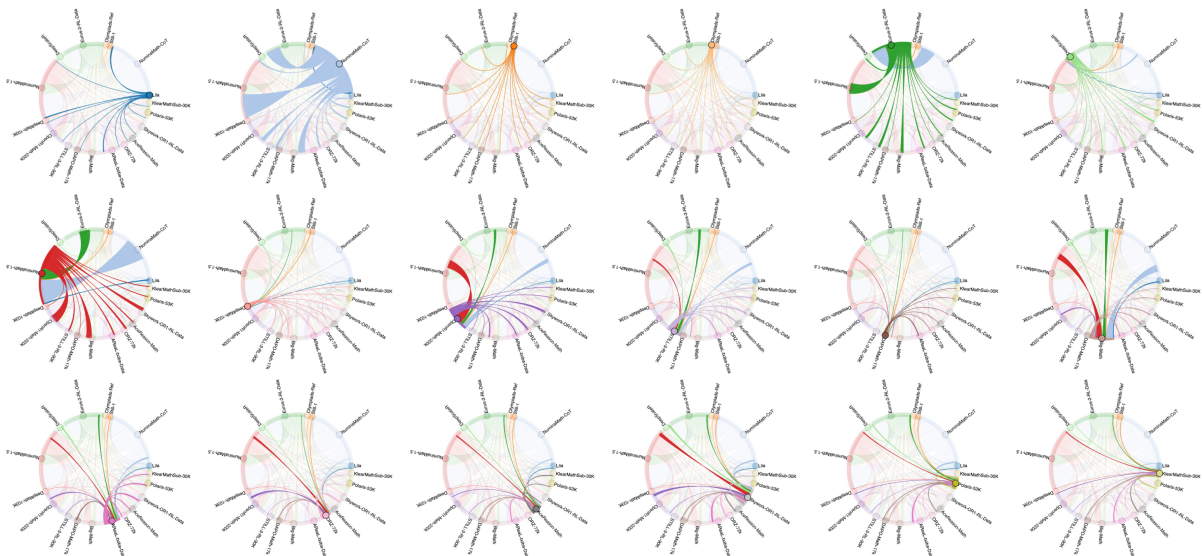


Figure 6: Bokeh plots visualizing the compositional relationships and data overlaps among different RLVR datasets.

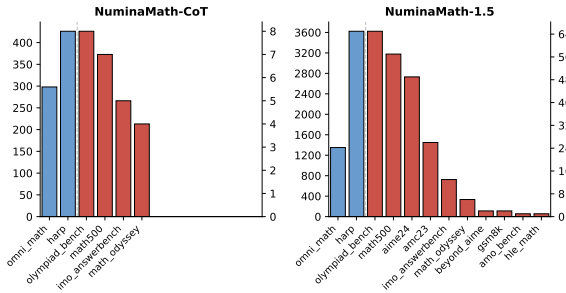


Figure 7: Benchmark leakage statistics of main source datasets, measured by semantic overlap.

B.2 Leakage Case Studies

Table 8 presents representative case studies of benchmark leakage identified through our lineage-aware tracing and semantic matching pipeline.

C Details of RLVR Dataset Benchmarking

C.1 What Makes Good RLVR Data?

We evaluate RLVR data from two complementary perspectives: **Static Quality** and **Dynamic Utility**.

Static Quality. Static Quality measures the intrinsic properties of an instance and whether it provides reliable and informative supervision signals. We consider three criteria: (1) **Verifiability**: Answers should be unambiguous and automatically verifiable, such that identical prompts should not correspond to conflicting answers. Open-ended formats are generally preferred over multiple-choice questions (MCQs), whose answers may be guessed without genuine reasoning. (2) **Learnability**: samples should provide meaningful learning signals, avoiding problems that are overly easy or overly difficult. (3) **Low Contamination**: training data should have minimal overlap with evaluation benchmarks, including both exact duplicates and semantically similar problems.

Dynamic Utility. Dynamic Utility evaluates whether the instance from a particular atomic source leads to actual performance gains after RLVR training while independent of test set. Assessing with a held-out benchmark, we consider two metrics: (1) **Sampling Efficiency Gain**: the improvement in sampling efficiency of the RL-aligned model relative to the base model, measured by the increase in Mean@N. (2) **Capability Boundary Expansion**: the extent to which RL training enables the model to solve previously un-

solved problems relative to the base model, measured by improvements in Pass@N.

C.2 Details of Implementation

Training Settings For RL finetuning, we use the widely adopted GRPO algorithm built on *VERL* (Sheng et al., 2025) framework. The full hyperparameters used in our training are listed in Table 9. Specifically, for rollout generation, we use a temperature of 1.0, and rewards are computed using *Math-Verify*. All models are trained for $T = 500$ optimization steps, and we report results using *Math500* as validation set to select best checkpoint.

Hyper-parameter	Value
Learning Rate	1e-6
Total Steps	500
Batch Size	128
Mini Batch Size	64
KL Loss Coefficient	0.0
Clip Ratio	0.2
Temperature	1.0
Total Number of Rollouts	8
Maximum Prompt Length	4096
Maximum Response Length	16384

Table 9: Full hyper-parameters for training.

Evaluation Settings For all evaluations, we use a decoding temperature of 0.6 with top_p=0.95, top_k=20, a maximum generation length of 16384 tokens, and a fixed random seed of 0. For the AMC23, AIME24, AIME25, and AMO benchmarks, which contain relatively small test sets, we report *Mean@32* (for *Pass@1*), while for the remaining benchmarks we report *Mean@4* (for *Pass@1*).

C.3 OOD Results

In addition to mathematical reasoning benchmarks, we also evaluate our method on out-of-domain (OOD) datasets, including the general QA benchmark GPQA, with results shown in Table 10.

Model	Biology	Physics	Chemistry	Overall
<i>Qwen3-1.7B-Base</i>	32.9	28.5	30.1	29.7
↔ DeepScaleR	43.4	29.7	34.1	33.1
↔ DeepMath	48.7	39.2	42.5	41.7
↔ OpenR1	34.2	27.3	33.9	31.1
↔ DAPO	44.7	33.1	35.8	35.5
↔ Skywork	36.8	35.2	38.2	36.7
↔ DAPO++ (ours)	42.1	34.0	36.3	35.9
<i>Qwen3-8B-Base</i>	60.5	45.9	37.9	43.6
↔ DeepScaleR	56.6	47.1	33.9	41.8
↔ DeepMath	60.5	58.7	33.3	47.0
↔ OpenR1	61.8	39.8	40.9	42.4
↔ DAPO	51.3	68.9	40.9	54.0
↔ Skywork	65.8	52.9	41.9	49.0
↔ DAPO++ (ours)	65.8	68.0	41.7	55.4

Table 10: Mean@N results on the GPQA benchmark.

C.4 SCA Results

We report the evaluation *Mean@N* results (Table 11) and *Pass@N* results (Table 12) of RLVR checkpoints trained on individual atomic sources identified by ATLAS. Following prior RLVR evaluation practice, we use *Math500* as the validation set and treat its performance as a proxy signal for our dataset scoring framework in Section §3.2.

C.5 Hyperparameter Settings

We provide the hyperparameter settings used for benchmarking in Table 13. All hyperparameters were selected through grid search.

Description. For the verifiability-related coefficients, α_{con} controls the weight of the consistency score R_{con} , α_{mcq} and β_{mcq} jointly determine the strength of the MCQ penalty term, and α_{reuse} controls the reuse discount factor P_{reuse} . For the static quality score S_1 , the weights w_{1a} , w_{1b} , and w_{1c} correspond to the contributions of verifiability, learnability, and contamination, respectively. The α coefficients are shared across L_{SCA} , the learnability term S_{1b} , and the proxy objectives for S_2 and S_3 . Specifically, α_{01} represents the gold-signal reward, α_{11} corresponds to the too-easy penalty, α_{10} models the base-competence signal, and α_{00} controls the too-hard penalty. Finally, the composite quality score Q is formed by aggregating static quality (S_1), sampling efficiency (S_2), and capability expansion (S_3) using weights w_1 , w_2 , and w_3 , respectively.

Parameter	1B	8B
S_{1a} coefficients: Verifiability-related scoring terms		
α_{con}	0.50	0.50
α_{mcq}	0.30	0.30
β_{mcq}	0.50	0.50
α_{reuse}	0.20	0.20
S_1 weights: Static dataset quality composition		
w_{1a}	0.20	0.20
w_{1b}	0.55	0.50
w_{1c}	0.25	0.30
α coefficients: SCA-based learnability utilities		
α_{01}	-0.3	+1.5
α_{11}	-0.5	-0.8
α_{10}	+1.5	+0.5
α_{00}	-1.5	-0.8
Composite Q weights: Final dataset quality aggregation		
w_1	0.50	0.35
w_2	0.30	0.35
w_3	0.20	0.30

Table 13: Hyperparameters for the RLVR Dataset Quality Score Q . Scale-dependent values are given for two representative model sizes; intermediate values are obtained by linear interpolation in $\log_{10}(M/1B)$.

D Related Work

Recent surveys have highlighted the growing importance of data provenance, traceability, and transparency in LLMs (Hohensinner et al., 2026), emphasizing the increasing opacity of modern training corpora and the need for provenance-aware AI systems. However, existing work has rarely investigated in the RLVR setting, particularly at the level of *atomic sources*. Prior studies have instead focused primarily on data contamination tracing and contamination detection in LLMs (Cheng et al., 2025; Fu et al., 2025).

Moreover, our work also studies RLVR datasets from a benchmarking perspective. While dataset benchmarking has recently attracted increasing attention, existing efforts mainly focus on evaluating *test benchmarks* rather than *training datasets*. For example, Benchmark² (Qian et al., 2026) systematically evaluates the quality of LLM benchmarks from perspectives such as ranking consistency, discrimination ability, and capability-level alignment, revealing reliability and separability issues in existing evaluation benchmarks. Similarly, Benchmark Health Index (Zhu et al., 2026) proposes a data-driven framework for assessing benchmark quality and longevity through discrimination power, anti-saturation capability, and ecosystem impact. In contrast, our work focuses on benchmarking RLVR training datasets through source-aware lineage tracing and counterfactual utility estimation.

Training Set	Test Set
Case 1: DeepScaleR-Preview-Dataset (omni_math) vs math500 (sim = 0.9821)	
<p>Prompt: Consider the function $z(x, y)$ describing the paraboloid $z = (2x - y)^2 - 2y^2 - 3y$. Archimedes and Brahmagupta are playing a game. Archimedes first chooses x. Afterwards, Brahmagupta chooses y. Archimedes wishes to minimize z while Brahmagupta wishes to maximize z. Assuming that Brahmagupta will play optimally, what value of x should Archimedes choose?</p> <p>Answer: $-\frac{3}{8}$</p>	<p>Prompt: Consider the function $z(x, y)$ describing the paraboloid $z = (2x - y)^2 - 2y^2 - 3y$. Archimedes and Brahmagupta are playing a game. Archimedes first chooses x. Afterwards, Brahmagupta chooses y. Archimedes wishes to minimize z while Brahmagupta wishes to maximize z. Assuming that Brahmagupta will play optimally, what value of x should Archimedes choose?</p> <p>Answer: $-\frac{3}{8}$</p>
Case 2: DAPO-Math-17k (areal_boba) vs olympiad_bench (sim = 0.9818)	
<p>Prompt: Let \mathcal{A} denote the set of all polynomials in three variables x, y, z with integer coefficients. Let \mathcal{B} denote the subset of \mathcal{A} formed by all polynomials which can be expressed as $(x + y + z)P(x, y, z) + (xy + yz + zx)Q(x, y, z) + xyzR(x, y, z)$ where $P, Q, R \in \mathcal{A}$. Find the smallest non-negative integer n such that $x^i y^j z^k \in \mathcal{B}$ for all non-negative integers i, j, k satisfying $i + j + k \geq n$.</p> <p>Answer: 4</p>	<p>Prompt: Let \mathcal{A} denote the set of all polynomials in three variables x, y, z with integer coefficients. Let \mathcal{B} denote the subset of \mathcal{A} formed by all polynomials which can be expressed as $(x + y + z)P(x, y, z) + (xy + yz + zx)Q(x, y, z) + xyzR(x, y, z)$ with $P, Q, R \in \mathcal{A}$. Find the smallest nonnegative integer n such that $x^{(i)}y^{(j)}z^{(k)} \in \mathcal{B}$ for all nonnegative integers i, j, k satisfying $i + j + k \geq n$.</p> <p>Answer: 4</p>
Case 3: DeepMath-103K (stack_exchange) vs beyond_aimc (sim = 0.9233)	
<p>Prompt: Let the real numbers $x_1, x_2, \dots, x_{1997}$ satisfy the following conditions: (1) $-\frac{1}{\sqrt{3}} \leq x_i \leq \sqrt{3}$ for $i = 1, 2, \dots, 1997$; (2) $x_1 + x_2 + \dots + x_{1997} = -318\sqrt{3}$. Find the maximum value of $x_1^{12} + x_2^{12} + \dots + x_{1997}^{12}$.</p> <p>Answer: 189548</p>	<p>Prompt: Real numbers $x_1, x_2, \dots, x_{1997}$ satisfy the following two conditions: (1) $-\frac{1}{\sqrt{3}} \leq x_i \leq \sqrt{3}$ ($i = 1, 2, \dots, 1997$); (2) $x_1 + x_2 + \dots + x_{1997} = -318\sqrt{3}$. Let M be the maximal possible value of $x_1^{12} + x_2^{12} + \dots + x_{1997}^{12}$. Find the largest integer no more than M.</p> <p>Answer: 189548</p>
Case 4: Big-Math-RL-Verified-Processed (omni_math) vs imo_answerbench (sim = 0.9002)	
<p>Prompt: Sir Alex plays the following game on a row of 9 cells. Initially, all cells are empty. In each move, Sir Alex is allowed to perform exactly one of the following two operations: (1) Choose any number of the form 2^j, where j is a non-negative integer, and put it into an empty cell. (2) Choose two (not necessarily adjacent) cells with the same number in them; denote that number by 2^j. Replace the number in one of the cells with 2^{j+1} and erase the number in the other cell. At the end of the game, one cell contains 2^n, where n is a given positive integer, while the other cells are empty. Determine the maximum number of moves that Sir Alex could have made, in terms of n.</p> <p>Answer: $2 \sum_{i=0}^8 \binom{n}{i} - 1$</p>	<p>Prompt: Sir Alex plays the following game on a row of 9 cells. Initially, all cells are empty. In each move, Sir Alex is allowed to perform exactly one of the following two operations: (1) Choose any number of the form 2^j, where j is a non-negative integer, and put it into an empty cell. (2) Choose two (not necessarily adjacent) cells with the same number in them; denote that number by 2^j. Replace the number in one of the cells with 2^{j+1} and erase the number in the other cell. During the game, Sir Alex encounters a mysterious genie that grants him a wish. However, the genie warns Sir Alex that he can only make a limited number of moves. At the end of the game, one cell contains the number 2^{40}, while the other cells are empty. Determine the maximum number of moves that Sir Alex could have made.</p> <p>Answer: 200293447</p>

Table 8: Representative high-similarity cases between evaluation benchmarks and training data. Formatting differences are explicitly visualized using colored whitespace ($_$), newline tokens (\n), and display-math markers ($\[/math>/ $\]$). In both cases, the semantic content and final answers are identical, while differences are purely superficial formatting artifacts.$

Source	Mean@4				Mean@32				Average
	Math500	Minerva	Olympiad	HLE	AMC23	AIME24	AIME25	AMO	
<i>Qwen3-1.7B-Base</i>	48.4	15.3	17.6	5.9	28.2	4.7	2.3	1.3	15.5
gsm8k	25.9	5.2	9.1	2.5	13.4	2.5	1.0	0.9	7.6
olympiads	57.8	22.3	23.1	6.1	35.1	5.3	5.2	2.1	19.6
areal_boba	57.8	23.2	22.1	6.8	37.0	7.3	2.0	1.6	19.7
still3	60.4	25.0	23.7	5.3	31.6	6.5	4.7	0.8	19.7
synthetic_amc	56.9	22.9	21.8	7.6	36.9	5.5	3.5	2.1	19.7
aops_forum	56.8	21.4	22.0	5.5	38.5	7.1	5.2	1.8	19.8
stack_exchange	58.3	22.7	21.8	8.0	34.5	6.4	4.5	2.4	19.8
basic_arithmetic	58.5	22.8	23.4	6.1	36.7	6.2	4.6	1.9	20.0
num_glue	58.8	22.1	22.9	7.2	36.8	5.4	4.6	2.0	20.0
still1	59.0	22.3	23.1	5.1	38.7	5.8	3.4	2.4	20.0
dapo	58.5	21.5	23.0	5.5	39.8	8.3	4.4	1.6	20.3
lila_crawl	59.0	22.5	23.6	6.2	37.7	7.9	4.5	1.8	20.4
amc_aime	58.7	23.0	23.6	7.0	36.8	8.4	4.3	1.9	20.5
lila_synthetic	60.4	23.8	24.7	4.3	36.5	6.9	5.7	1.8	20.5
math	60.3	23.9	<u>25.8</u>	4.7	39.5	5.4	3.8	1.4	20.6
meta_math	58.5	24.2	23.1	7.4	37.3	7.0	<u>5.6</u>	1.8	20.6
big_math	59.6	23.9	25.0	5.3	40.2	6.8	2.7	1.8	20.7
numina_math1.5	58.2	23.3	23.9	6.8	40.7	7.5	3.3	3.2	20.9
test_leak	59.8	23.6	23.9	5.5	<u>42.7</u>	7.8	4.2	1.5	21.1
cn_k12	59.4	<u>24.8</u>	24.0	4.3	41.6	9.3	4.1	2.1	21.2
orca_math	60.0	22.5	25.0	5.9	42.8	8.3	4.6	1.8	<u>21.4</u>
synthetic_math	60.5	<u>24.8</u>	26.5	6.1	41.6	<u>9.1</u>	3.5	<u>2.9</u>	21.9

Table 11: Mean@N results of RL checkpoints trained with different atomic source datasets under the SCA setting. Relative to Qwen3-1.7B-Base, improvements (blue) and degradations (red) are color-coded by intensity, respectively.

Source	Pass@4				Pass@32				Average
	Math500	Minerva	Olympiad	HLE	AMC23	AIME24	AIME25	AMO	
<i>Qwen3-1.7B-Base</i>	66.6	28.7	28.7	17.2	80.0	33.3	23.3	8.0	35.7
gsm8k	42.2	10.7	18.7	9.4	60.0	30.0	20.0	<u>10.0</u>	25.1
still3	<u>71.8</u>	33.5	33.3	11.7	75.0	26.7	16.7	8.0	34.6
areal_boba	68.4	33.5	34.1	14.1	77.5	20.0	20.0	12.0	34.9
amc_aime	69.6	34.2	32.4	15.6	77.5	30.0	23.3	6.0	36.1
math	70.0	33.5	35.3	12.5	80.0	23.3	23.3	12.0	36.2
numina_math1.5	70.4	33.1	33.9	14.8	82.5	30.0	13.3	12.0	36.3
synthetic_amc	71.2	34.6	32.7	18.0	77.5	26.7	23.3	<u>10.0</u>	36.7
still1	69.6	33.5	32.6	11.7	80.0	<u>33.3</u>	23.3	12.0	37.0
orca_math	71.2	31.6	36.3	11.7	80.0	26.7	<u>30.0</u>	<u>10.0</u>	37.2
num_glue	70.2	33.5	33.3	<u>17.2</u>	75.0	30.0	26.7	12.0	37.2
stack_exchange	69.4	32.4	32.6	18.0	77.5	36.7	23.3	<u>10.0</u>	37.5
lila_synthetic	<u>71.8</u>	34.2	35.0	11.7	75.0	<u>33.3</u>	<u>30.0</u>	<u>10.0</u>	37.6
aops_forum	71.2	30.9	34.1	14.1	80.0	36.7	26.7	8.0	37.7
dapo	71.2	32.7	35.9	14.8	80.0	26.7	<u>30.0</u>	<u>10.0</u>	37.7
big_math	71.4	34.9	<u>36.7</u>	14.1	80.0	30.0	23.3	12.0	37.8
meta_math	69.0	<u>35.3</u>	35.4	18.0	77.5	<u>33.3</u>	26.7	8.0	37.9
test_leak	70.0	33.8	34.4	13.3	<u>85.0</u>	30.0	26.7	<u>10.0</u>	37.9
synthetic_math	71.0	33.5	39.0	15.6	72.5	<u>33.3</u>	26.7	12.0	37.9
basic_arithmetic	69.8	33.8	35.9	14.8	<u>85.0</u>	26.7	<u>30.0</u>	8.0	38.0
lila_crawl	70.6	32.4	35.6	16.4	82.5	<u>33.3</u>	23.3	<u>10.0</u>	38.0
olympiads	70.6	34.6	35.4	15.6	<u>85.0</u>	30.0	<u>30.0</u>	<u>10.0</u>	<u>38.9</u>
cn_k12	72.0	36.8	36.6	11.7	87.5	<u>33.3</u>	36.7	12.0	40.8

Table 12: Pass@N results of RL checkpoints trained with different atomic source datasets under the SCA setting. Relative to Qwen3-1.7B-Base, improvements (blue) and degradations (red) are color-coded by intensity, respectively.